Automatic Coronary Angiogram Keyframe Extraction

Hounaida Moalla[1,2] [a], Aiman Ghrab[3] [b], Bassem Ben Hamed[2,4] [c], Amine Bahloul[3] [d],
Rania Hammami[3] [e] and Leila Abid[3] [f]

[1]*Higher Institute of Technological Studies, University of Sfax, Sfax, Tunisia*

fi

[3]*Hedi Chaker University Hospital of Sfax, University of Sfax, Sfax, Tunisia*

[4]*National School of Electronics and Telecommunications of Sfax, University of Sfax, Sfax, Tunisia*

Keywords: Coronary Angiograms, Keyframes, Filters.

Abstract: Coronary artery disease is one of the most feared atherosclerosis complications. Doctors use coronary angiography as a diagnostic tool to diagnose a patient with obstructive coronary artery disease and treat it efficiently. The effectiveness of the doctor's intervention strongly depends on the quality of the diagnosis. Therefore, good extraction of keyframes from coronary angiography will certainly improve the accuracy of the decision. Hence the importance is given to this step. To determine the best way to extract keyframes from coronary angiograms, we tested several methods for keyframe extraction. Our keyframe extraction method that we propose is based on the use of filters and the calculation of frame intensities of a given coronary angiogram. The pilot frame is the brightest one, and the keyframes will be its six neighboring frames. Our method Contrast Enhanced Sato filter, succeeded in extracting the right keyframes with an accuracy of around 85.74%.

1 INTRODUCTION

Coronary artery disease is the first cause of mortality and morbidity in developed countries and worldwide (Ojha and Dhamoon, 2021). This recent increase in this disease is secondary mainly to one's health style and to the development of diagnostic tools (Lee et al., 2022). Coronary angiography remains the best diagnostic method for obstructive coronary artery disease (CAD). However, it has some limitations: clinicians often use visual assessment to assess the severity of a coronary plaque obstruction. This method is the source of interobserver variability. Accurate estimation is of great importance because it will lead to treatment strategies such as Percutaneous Coronary Intervention (PCI), Coronary Artery Bypass Graft (CABG) surgery, or simply medical treatment (Neumann et al., 2019). To mitigate these lim-

itations, the constructors of Catheterization laboratory (Cath lab) equipment provide many solutions: a simple method is Quantitative Coronary Angiography analysis (QCA) (Collet et al., 2017). QCA is a great tool because it estimates obstruction percentage and the artery reference diameter by semi-automatic keyframe analysis. It requires third-party manual input, the clinician, or the Cath lab technician. Even though this method decreases interobserver variability, it still has poor reproducibility (Avram et al., 2021). Fully automated analysis solutions are still in the development stage and have not yet been implemented in Cath labs. To extract information from an angiogram, a sequence of X-ray captured images, determining the keyframe is the first and most important step because it will affect the analysis. In this work, we try to determine the most efficient method of keyframe extraction.

For technical reasons, X-Ray Angiogram (XRA) has low contrast between vessels and background, many artifacts (such as bony structures, pacemaker leads, ...), image noise, and non-uniform illumination (Kerkeni et al., 2016). All these characteristics make automatic recognition of vascular structures a hard task. It is, therefore, necessary to improve the

[a] https://orcid.org/0000-0003-3180-9446
[b] https://orcid.org/0000-0002-1974-9551
[c] https://orcid.org/0000-0003-1586-9537
[d] https://orcid.org/0000-0003-1632-5646
[e] https://orcid.org/0000-0003-1168-6450
[f] https://orcid.org/0000-0001-7793-5240

quality of these images by applying enhancing algorithms (increasing contrast, noise reduction...) as a first step.

The last decade has been marked by the evolution of computing techniques in imaging thanks to new hardware (memory capacity, processing speed,...), software (new languages, specific applications,...), and architectural technologies that are efficient and easy to use. All these advantages have been widely exploited in the medical field, particularly in the detection of stenoses by image processing.

In the literature, several approaches to preprocessing have been proposed. They consist of tracing the borders of the vessels more clearly to be as precise as possible when determining the vascular volume (Danilov et al., 2021; Lamy et al., 2021). These methods are mainly based on the application of filters. The choice of filters highly depends on the dataset and the quality of the images to be processed.

This paper demonstrates the results of different filter-based algorithms applied to a coronary angiogram dataset and assesses them to determine the most efficient algorithm.

2 RELATED WORKS

Video processing can consist of finding the keyframe using different techniques such as motion-based information gathering, video frame aggregation, and shot detection. On the other hand, the classic keyframe identification algorithms (in their raw states) do not perform well in the processing of coronary angiography videos. that's why adaptations to the field of application are useful (Kavipriya and Hiremath, 2022). In fact, in recent research about automatic coronary angiogram analysis, few acceptable solutions were found. This may be due to the characteristics of X-ray acquisitions (Kerkeni et al., 2016).

Since a keyframe is defined as a frame that contains a vessel full of dye, some authors used vessel extraction to identify it. Moon et al. (Moon et al., 2021) automated keyframe detection method used this definition: first, they applied a contrast enhancing treatment using a multi-scale top-hat transform-based algorithm, then, vessel structure was extracted using a Frangi filter: the keyframe was defined as the one the highest number of surviving pixels. Avram et al. (Avram et al., 2021) used a similarity index, a parameter that translates the difference between each frame and the first frame (empty vessel). The keyframe is the one with the lowest index.

On the other hand, Zhou et al. (Zhou et al., 2021) used a two-phase algorithm to train a deep learning keyframe classification model using a manually labeled database. They used a ResNet 18 architecture and a combination of neural network optimizers.

Keyframe extraction is based on image processing techniques to detect the vessels. This process is preceded by applying filters on the images to increase the contrasts (Zhou et al., 2021). The choice of the adequate filter is not based on standard rules but rather empirical, depending on the images' quality and the dataset used (Lamy et al., 2021). The first comparative study of several filters was proposed by (Lamy et al., 2021) such as Frangi, Sato, and Canny. Another filter research was conducted by (Sazak et al., 2019) to compare Hessian filters, Phase Congruency Tensor (PCT), and mathematical morphology-based method.

(Qin et al., 2022) do not filter images but suggest a new method for extracting vessels from coronary angiography images. Their architecture is based on a PCA unrolling network containing a pooling layer and a long-term convolutional memory network.

On the other hand, the choice of keyframes has been discussed in several previous works (Kerkeni et al., 2016; Lamy et al., 2021; Gawande et al., 2020) based on the calculations of intensity, similarity, distance, histograms, clustering,... Other means that are also useful consist of applying deep learning models to extract keyframes by eliminating those with great similarities (Gawande et al., 2020). A combination of the two strategies has also been proposed in (Jo et al., 2018).

Closer to the domain, the process of extracting keyframes depends on the context: it can mean extracting a summary of a sequence of images. Therefore it chooses frames that sum up the whole sequence, just like film processing (Thakre et al., 2016; Gawande et al., 2020; Jiang and Shi, 2021). Extraction can also focus on a sample of frames containing the maximum amount of data; we can cite the example of medical angiograms (Zhou et al., 2021; Gawande et al., 2020). These two have been the subject of several studies. The algorithms that have been proposed eventually depend on the subject.

3 LITERATURE OF USED METHODS

3.1 Hessian Filter

Most filtering methods are based on the calculation of image intensity. The calculation of the Hessian matrix then turns out to be the best method to give more performance. For a 3D input image, the Hessian matrix is a 3×3 matrix composed of second-order partial

derivatives of the input image. At each point of the image, Hessian matrix H is a function f(x1, x2, x3) defined as in (1):

$$H(f) = \begin{bmatrix} h_{11} & h_{12} & h_{13} \\ h_{21} & h_{22} & h_{23} \\ h_{31} & h_{32} & h_{33} \end{bmatrix} = \begin{bmatrix} \frac{\partial^2 f}{\partial x_1^2} & \frac{\partial^2 f}{\partial x_1 \partial x_2} & \frac{\partial^2 f}{\partial x_1 \partial x_3} \\ \frac{\partial^2 f}{\partial x_2 \partial x_1} & \frac{\partial^2 f}{\partial x_2^2} & \frac{\partial^2 f}{\partial x_2 \partial x_3} \\ \frac{\partial^2 f}{\partial x_3 \partial x_1} & \frac{\partial^2 f}{\partial x_3 \partial x_2} & \frac{\partial^2 f}{\partial x_3^2} \end{bmatrix}$$

(1)

Hessian then applies a Gaussian kernel of standard deviation σ to convolve the initial images. A blood vessel will then be seen as a clear tube against a dark background. Several filters are derived from Hessian in order to improve the visibility of vessels such as Sato, Canny, and Meijering.

3.2 Sato Filter

Sato is a method to improve the visibility of curvilinear structures such as vessels and bronchi in 2D and 3D medical images (Sato et al., 1998). It is a vessel enhancement approach based on the eigenvectors of the Hessian matrix aimed at both the discrimination of linear structures from other structures and the recovery of the original linear structures from the corrupted structures. (2) expresses the Sato filter:

$$F = \begin{cases} \lambda_c exp\left(\frac{-\lambda_1^2}{2(\alpha_1 \lambda_c)^2}\right) & : \lambda_1 \leq 0, \lambda_c \neq 0 \\ \lambda_c exp\left(\frac{-\lambda_1^2}{2(\alpha_2 \lambda_c)^2}\right) & : \lambda_1 \geq 0, \lambda_c \neq 0 \\ 0 & : \lambda_c = 0 \end{cases}$$

(2)

with

$$\lambda_c = min(-\lambda_2, -\lambda_3)$$

(3)

3.3 Meijering Filter

The Meijering filter is a vessel function developed to detect vascular structures. This approach was initially proposed for 2D images (Meijering et al., 2004) and then extended to 3D (Obara et al., 2012). It is also based on the modified Hessian matrix defined by (4):

$$H(f) = \begin{bmatrix} h_{11} + \frac{\alpha}{2}(h_{22} + h_{33}) & (1 - \frac{\alpha}{2})h_{12} & (1 - \frac{\alpha}{2})h_{13} \\ (1 - \frac{\alpha}{2})h_{21} & h_{22} + \frac{\alpha}{2}(h_{11} + h_{33}) & (1 - \frac{\alpha}{2})h_{23} \\ (1 - \frac{\alpha}{2})h_{31} & (1 - \frac{\alpha}{2})h_{32} & h_{33} + \frac{\alpha}{2}(h_{11} + h_{22}) \end{bmatrix}$$

(4)

The Meijering filter is then defined as in (5):

$$F = \begin{cases} \lambda_{max}/\lambda_{min} & : \lambda_{max} \leq 0 \\ 0 & : \lambda_{max} \geq 0 \end{cases}$$

(5)

where

$$\lambda_{max} = max(\lambda_1', \lambda_2', \lambda_3')$$

(6)

is computed at each voxel.

3.4 Frangi Filter

This filter can also detect continuous ridges, such as rivers, ripples, and ships in 2D and 3D images (Frangi et al., 1998). It computes Hessian eigenvectors to calculate the similarity of an image region to vessels. The method relies on the use of three vectors to be more discriminating. Three measures are derived from these eigenvectors as shown in (7):

$$R_b = |\lambda_1|/\sqrt{|\lambda_2 \lambda_3|}$$
$$R_a = |\lambda_2|/|\lambda_3|$$
$$S = \sqrt{\lambda_1^2 + \lambda_2^2 + \lambda_3^2}$$

(7)

Where Rb is the blob-like structure measure and S is the Frobenius norm of the Hessian matrix. These measures are combined in a vesselness function as given by (8):

$$V_\sigma(p) = |x| = \begin{cases} 0 & if \lambda_2 \leq 0 \\ exp(-\frac{R_b^2}{2\beta^2})(1 - exp(-\frac{S^2}{2c^2})) & otherwise \end{cases}$$

(8)

where β and c are thresholding parameters to control the sensitivity of the filter to Rb and S respectively.

3.5 Canny Filter

It is a multi-step algorithm (Canny, 1986) :

- Noise reduction: this step is based on the application of the Gaussian filter to remove the noise. The equation for a Gaussian filter kernel of size (2k+1)×(2k+1) is given as in (9):

$$H_{ij} = \frac{1}{2\pi\sigma^2} exp(-\frac{(i-(k+1))^2 + (j-(k+1))^2}{2\sigma^2})$$

(9)

with $1 \leq i, j \leq (2k+1)$.

The selection of the Gaussian kernel size will influence the performance of the detector. A small size corresponds to a powerful sensitivity to noise. A 5x5 or 3x3 can be good choices depending on the input.

- Gradient calculation: computing intensity and direction of edges by calculating the gradient of the image applying edge detection operators. The change in intensity of the pixels can mean the existence of edges whose detection can be done by applying Sobel filters to show this change in intensity in both directions: horizontal (x) and vertical (y) as (10):

$$K_x = \begin{pmatrix} -1 & 0 & 1 \\ -2 & 0 & 2 \\ -1 & 0 & 1 \end{pmatrix}, K_y = \begin{pmatrix} 1 & 2 & 1 \\ 0 & 0 & 0 \\ -1 & -2 & -1 \end{pmatrix}$$

(10)

Then, the gradient is applied according to (11):

$$|G| = \sqrt{I_x^2 + I_y^2}$$
$$\theta(x,y) = arctan(\frac{I_y}{I_x}) \qquad (11)$$

- Non-maximal suppression: A full image analysis is performed to remove any unwanted pixels that may not constitute the edge. The result will be a binary image with "thin edges".

- And hysteresis threshold by setting two threshold values for the intensity gradient (minVal and maxVal) to detect the edges to keep and those to delete. Thresholds must simply be well chosen. Fig. 1(a) illustrates the effect of these filters on a coronary angiogram.

3.6 Stacked Filters

The result of the filters mentioned above are modest. For better output, we try the stack of filters. Adding a gaussian filter to a frame before or after the application of a Sato or a Frangi filter may lead to improved results thanks to its ability to remove the noise. Also, an after-treatment with a filter that improves the contrast could have much more outstanding outcomes. This is highlighted in Fig. 1(b).

4 PROPOSED METHOD

To develop a fully automated keyframe extraction method, we focused on vessel extraction techniques. We transformed angiogram videos into a sequence of frames. We then applied different vessel-enhancing algorithms to determine the frame that contains a vessel full of contract agents. Our contribution is summarized in the extraction of keyframes from an angiographic video based on the use of filters in order to improve the recognition of the heart vessels.

The filter technique in itself is not new, but the extraction algorithm we propose has given good results. In the first step, the set of filters we used was Canny, Meijering and Sato. Each time, we apply a filter from the list as shown in Algorithm 1.

```
#Algorithm 1: pre-treatment of frames
Algorithm Keyframes ( )
Begin
Input : set of frames
Output : list of keyframes
L=[ ]
for f in frames :
im=read(f)
gray=grayscale(im)
```

```
res=filter(gray)
int=intensity(res)
L_int.append(int)
M=max(L_int)
ind=L_int .index(M)
nb_k=7
keys=extract(ind, L_int,nb_k)
End.

#Algorithm 2: extraction of keyframes
Algorithm extract (ind, L_int, nb_k)
Begin
L_kf=[ ]
for i in range (ind-nb_k//2,ind+nb_k//2) :
if (i>0 and i < nb) :
frame=read(L_int[i])
L_kf.append(frame)
else :
pass
save ( L_kf )
End.
```

The Keyframes algorithm is run for each frame set of a separate angiographic video. At each frame, we apply the chosen filter, then we calculate the intensity of the filtered image. All the intensities are saved in a list. The pilot frame will be the one having the maximal intensity. From its position in the list, Algorithm 2 selects the 6 neighboring frames of the pilot frame.

Thereafter, to improve the results, we rounded the percentages of conformity compared to the manual annotation according to Algorithm 3.

```
#Algorithm 3: improvement of keyframes extraction
Algorithm improvement ( )
Begin
L_frames=liste of frames manually annotated
nbF=len(L_frames)
# iterate through the list of patients in the
datasets for p in patients :
pourcentagePatient=0
# iterate through the list of coros in the
dataset for c in coros :
Lf=liste of 6 keyFrames of the coro c
nb_fp=6
pourcentageCoro =0
n=0
for f in Lf :
if c in L_frames :
n+=1
if n > 4 :
pourcentageCoro=100
else :
pourcentageCoro = (nb_fp / nbF ) * 100
pourcentagePatient+=pourcentageCoro
pourcentagePatient = pourcentagePatient/nbCoro
pourcentageTotal+=pourcentagePatient
pourcentageTotal = pourcentageTotal / nbPatients
return pourcentageTotal
End.
```
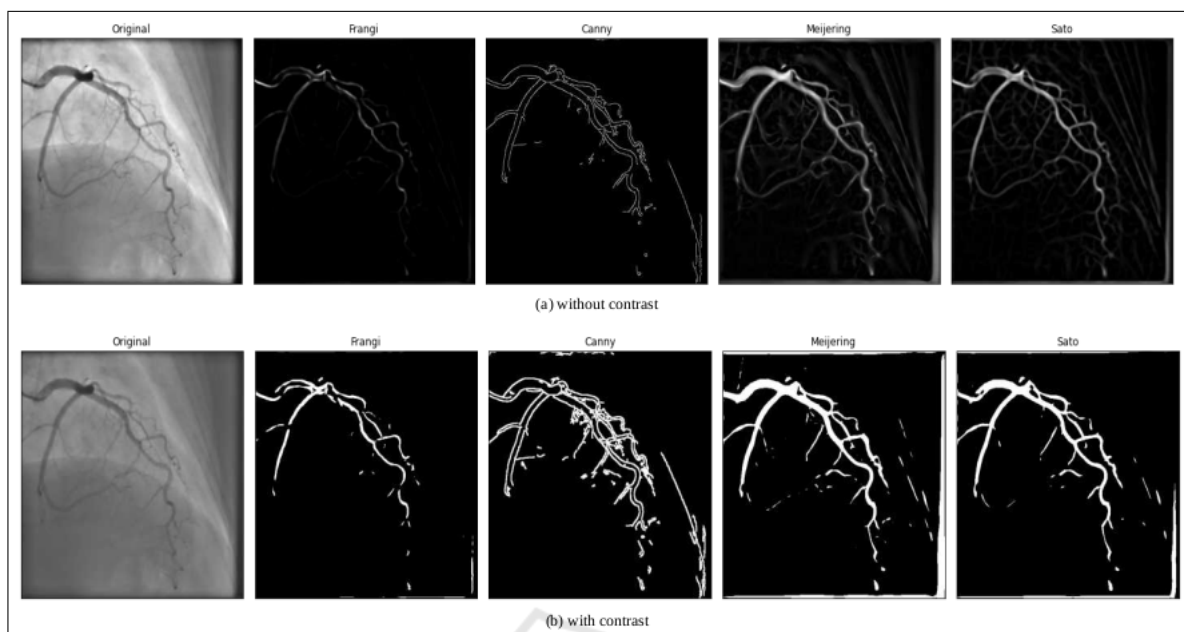
Figure 1: Original frame with results of filters.

5 EXPERIMENTAL RESULTS

5.1 Dataset

The full dataset was collected from exams performed by a single catheterization laboratory during the period between January 2018 and December 2021.
Dataset consisted of 3159 angiographic study: a total of 37209 coronary angiograms was extracted. We used a sample of 45 angiograms to extract a total of 1434 frames of size 512 x 512 pixels. We developed a web application to help two experienced cardiologists to annotate a sample from our dataset. The manual annotation found 474 keyframes and 960 non-keyframe. The frames were randomly split into 80% training and 20% test datasets.

5.2 Results of Vessel Extraction

In the first step, algorithms 1 and 2 were applied once on the original dataset without filters, then we tested them with filters. The results showed that the calculation with a fixed 6 keyframes gave the best result provided by the Sato filter: 77,58%. Using an improvement algorithm, we improved our results from 77.58% to 85.74%.
In the second step, we applied a pre-processing composed of two pipelined filters. We proposed to pre-execute the Gaussian filter on the frames before or after applying the filters mentioned above. The choice

of the Gaussian filter is justified by his ability to eliminate the noise of the images. The two-filters pipeline also gave acceptable results. Since angiograms usually have a thick black frame secondary to the acquisition parameters, a third optimization technique is to use a crop function. Cropping was applied once with a number of 50 pixels on all four sides, then again with a variable number of pixels.
Table 1 shows the keyframe extraction results using the proposed algorithm. Meijering gave the worst results even when combined with a gaussian filter. On the other hand, a Contrast-Sato had the best outcomes with an overall accuracy of 85.74%. Fig. 2 shows an example of the results obtained with each algorithm.
From these results, we conclude that cropping did not have a major effect on the results and the combination of filters seems to have an unpredictable outcome except for the contrast filter. Fig. 3 shows the intensity curve of the frames of the same example. Our Contrast-Sato algorithm produced the keyframes from 12 to 17. This set coincides with the manual annotation in 4 frames out of 6, therefore presenting a satisfactory result.

6 CONCLUSION

We have developed an algorithm for extracting keyframes from angiographic video sequences. The proposed method detected keyframes with an accu-

Table 1: Extraction percentages of keyframes using filters.

| Filters	With fixed number of frames				With a variable number of frames	
	Without cropping		With cropping		Without cropping	With cropping
	Without improvement	With improvement	Without improvement	With improvement		
Original images	19.01	20.08	38.39	40.80	16.68	37.89
Meijering	22.58	36.91	11.79	13.45	35.77	10.17
Canny	72.85	81.74	70.07	78.16	73.49	70.79
Sato	77.58	85.74	73.39	80.92	73.34	74.52
Canny-Gaussian	72.85	81.74	70.07	78.16	73.49	70.79
Gaussian-Canny	55.97	60.86	57.38	60.37	59.00	56.01
Meijering-Gaussian	33.58	36.91	11.79	13.45	35.77	10.17
Gaussian-Meijering	61.25	67.93	18.70	22.77	60.21	18.96
Sato-Gaussian	77.70	85.18	76.35	82.77	72.29	73.39
Gaussian-Sato	76.34	82.96	69.62	75.06	70.25	64.51
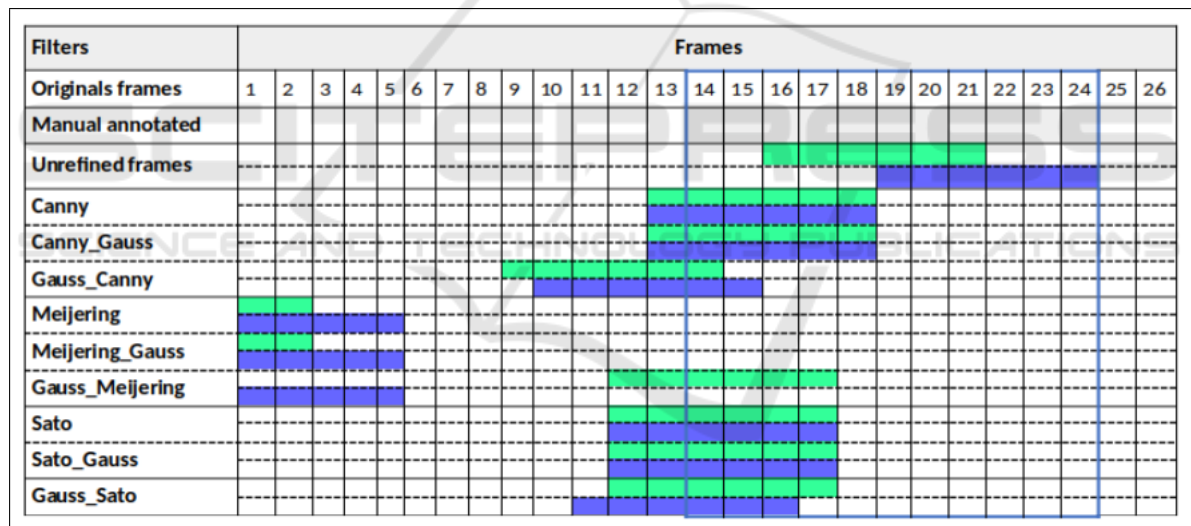
Figure 2: Keyframes extracted from a randomly drawn coro : (green) without cropping (blue) with cropping.

racy of 85.74% compared to manual annotation.

Greater attention will be devoted to this preliminary stage of processing the angiographic frames. Future improvements include the use of deep learning methods seeking closer performance.

REFERENCES

Avram, R., Olgin, J., Wan, A., Ahmed, Z., Verreault-Julien, L., Abreau, S., Wan, D., Gonzalez, J. E., So, D., Soni, K., et al. (2021). Cathai: Fully automated coronary angiography interpretation and stenosis detection using a deep learning-based algorithmic pipeline. *Journal of the American College of Cardiology*, 77(18_Supplement_1):3244–3244.

Collet, C., Grundeken, M. J., Asano, T., Onuma, Y., Wijns, W., and Serruys, P. W. (2017). State of the art: coronary angiography. *EuroIntervention: journal of EuroPCR in collaboration with the Working Group on Interventional Cardiology of the European Society of Cardiology*, 13(6):634–643.

Danilov, V. V., Klyshnikov, K. Y., Gerget, O. M., Kutikhin, A. G., Ganyukov, V. I., Frangi, A. F., and Ovcharenko, E. A. (2021). Real-time coronary artery stenosis detection based on modern neural networks. *Scientific*
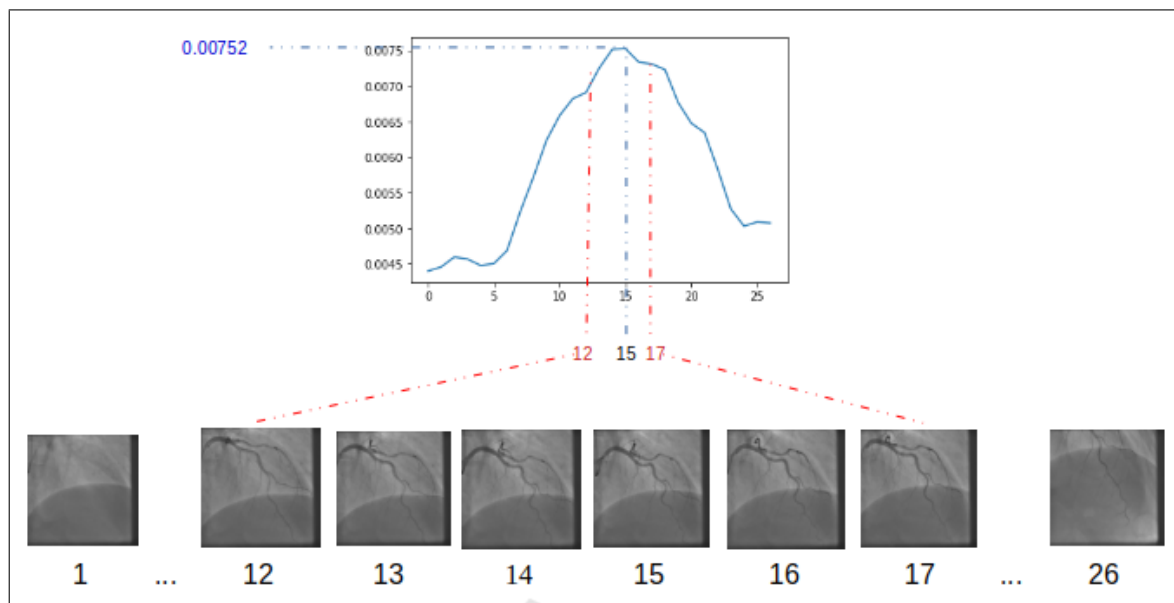
Figure 3: Temporal intensity score variation of coronary angiogram frames.

reports, 11(1):1–13.

Frangi, A. F., Niessen, W. J., Vincken, K. L., and Viergever, M. A. (1998). Multiscale vessel enhancement filtering. In *International conference on medical image computing and computer-assisted intervention*, pages 130–137. Springer.

Gawande, U., Hajari, K., and Golhar, Y. (2020). Deep learning approach to key frame detection in human action videos. *Recent Trends in Computational Intelligence*, 1:1–17.

Jiang, Z.-g. and Shi, X.-t. (2021). Application research of key frames extraction technology combined with optimized faster r-cnn algorithm in traffic video analysis. *Complexity*, 2021.

Jo, K., Kweon, J., Kim, Y.-H., and Choi, J. (2018). Segmentation of the main vessel of the left anterior descending artery using selective feature mapping in coronary angiography. *IEEE Access*, 7:919–930.

Kavipriya, K. and Hiremath, M. (2022). Computational method to extract the keyframe from angiogram video. *JOURNAL OF ALGEBRAIC STATISTICS*, 13(3):3088–3097.

Kerkeni, A., Benabdallah, A., Manzanera, A., and Bedoui, M. H. (2016). A coronary artery segmentation method based on multiscale analysis and region growing. *Computerized Medical Imaging and Graphics*, 48:49–61.

Lamy, J., Merveille, O., Kerautret, B., Passat, N., and Vacavant, A. (2021). Vesselness filters: A survey with benchmarks applied to liver imaging. In *2020 25th International Conference on Pattern Recognition (ICPR)*, pages 3528–3535. IEEE.

Lee, Y.-T. H., Fang, J., Schieb, L., Park, S., Casper, M., and Gillespie, C. (2022). Prevalence and trends of coronary heart disease in the united states, 2011 to 2018. *JAMA cardiology*, 7(4):459–462.

Meijering, E., Jacob, M., Sarria, J.-C., Steiner, P., Hirling, H., and Unser, e. M. (2004). Design and validation of a tool for neurite tracing and analysis in fluorescence microscopy images. *Cytometry Part A: the journal of the International Society for Analytical Cytology*, 58(2):167–176.

Moon, J. H., Cha, W. C., Chung, M. J., Lee, K.-S., Cho, B. H., Choi, J. H., et al. (2021). Automatic stenosis recognition from coronary angiography using convolutional neural networks. *Computer methods and programs in biomedicine*, 198:105819.

Neumann, F.-J., Sousa-Uva, M., Ahlsson, A., Alfonso, F., Banning, A. P., Benedetto, U., Byrne, R. A., Collet, J.-P., Falk, V., Head, S. J., et al. (2019). 2018 esc/eacts guidelines on myocardial revascularization. *European heart journal*, 40(2):87–165.

Obara, B., Fricker, M., Gavaghan, D., and Grau, V. (2012). Contrast-independent curvilinear structure detection in biomedical images. *IEEE Transactions on Image Processing*, 21(5):2572–2581.

Ojha, N. and Dhamoon, A. S. (2021). Myocardial infarction. In *StatPearls [Internet]*. StatPearls Publishing.

Qin, B., Mao, H., Liu, Y., Zhao, J., Lv, Y., Zhu, Y., Ding, S., and Chen, X. (2022). Robust pca unrolling network for super-resolution vessel extraction in x-ray coronary angiography. *IEEE Transactions on Medical Imaging*.

Sato, Y., Nakajima, S., Shiraga, N., Atsumi, H., Yoshida, S., Koller, T., Gerig, G., and Kikinis, R. (1998). Three-dimensional multi-scale line filter for segmentation and visualization of curvilinear structures in medical images. *Medical image analysis*, 2(2):143–168.

Sazak, Ç., Nelson, C. J., and Obara, B. (2019). The multi-scale bowler-hat transform for blood vessel enhancement in retinal images. *Pattern Recognition*, 88:739–750.

Thakre, K., Rajurkar, A., and Manthalkar, R. (2016). Video partitioning and secured keyframe extraction of mpeg video. *Procedia Computer Science*, 78:790–798.

Zhou, C., Dinh, T. V., Kong, H., Yap, J., Yeo, K. K., Lee, H. K., and Liang, K. (2021). Automated deep learning analysis of angiography video sequences for coronary artery disease. *arXiv preprint arXiv:2101.12505*.